# Wavelet Based Hilbert Transform with Digital Design and Application to QCM-SS Watermarking

*Santi Prasad MAITY*[1], *Seba MAITY*[2]

[1] Dept. of Information Technology, Bengal Engineering & Science Univ., Shibpur, Howrah-711 103, West Bengal, India,
[2] Dept. of Electronics & Communication Engineering, College of Engg. & Management, Kolaghat, West Bengal, India

santipmaity@it.becs.ac.in, seba_cemk@yahoo.co.in

**Abstract:** *In recent time, wavelet transforms are used extensively for efficient storage, transmission and representation of multimedia signals. Hilbert transform pairs of wavelets is the basic unit of many wavelet theories such as complex filter banks, complex wavelet and phaselet etc. Moreover, Hilbert transform finds various applications in communications and signal processing such as generation of single sideband (SSB) modulation, quadrature carrier multiplexing (QCM) and bandpass representation of a signal. Thus wavelet based discrete Hilbert transform design draws much attention of researchers for couple of years. This paper proposes an (i) algorithm for generation of low computation cost Hilbert transform pairs of symmetric filter coefficients using biorthogonal wavelets, (ii) approximation to its rational coefficients form for its efficient hardware realization and without much loss in signal representation, and finally (iii) development of QCM-SS (spread spectrum) image watermarking scheme for doubling the payload capacity. Simulation results show novelty of the proposed Hilbert transform design and its application to watermarking compared to existing algorithms.*

## Keywords

Hilbert transform, wavelets, biorthogonal wavelets, hardware design, QCM-SS watermarking.

## 1. Introduction

In signal analysis, Fourier transform is a potential tool that provides the mathematical basis for analyzing and designing frequency-selective filters to separate the signals on the basis of their frequency contents. Another method of separation of signals is done on the basis of *phase selectivity*, where phase shift between the pertinent signals are used to achieve the desired separation. Two values of phase shifts are of significant importance, one is shifting the phase angles of all components of a given signal by 180 degrees that requires the use of an ideal transformer, and the other one is ± 90 degrees that results a function in the original space or time domain known as Hilbert transform of the signal [1]. Hilbert transform can be applied to any signal that is Fourier transformable. Accordingly, Hilbert transform may be applied to energy signals as well as power signals. This leads to several important applications of Hilbert transform namely single sideband modulation (SSB), quadrature carrier multiplexing (QCM) and bandpass representation of signals [2].

Recently discrete wavelet transform (DWT) of 2-band decomposition along with its various variants like M-band wavelets and wavelet Packets find wide applications for detection, de-noising, and compression of multimedia signal etc. due to their better space-frequency localization, multi-resolution representation, superior HVS (human visual modeling) and adaptivity [3]. Various other versions of wavelets bases like *bandelet*, *curvilet* and *ridgelet* [4] are also found in very recent literature for efficient geometric representation and sharp image transition such as edges etc. Digital image and video watermarking is another interesting application of wavelets that has drawn attention of a group of researchers [5]. Watermarking is a technique where auxiliary information (watermark) is embedded into the original signals to serve ownership verification, copyright protection, authentication, integrity verification and access control etc. It is expected that data embedding process would not degrade perceptual quality of the original image and video signals (imperceptibility) and watermark information must be retained after various signal-processing operations (robustness) done over the watermarked signal [6]. Literature on wavelet domain watermarking for multimedia signals is quite rich [5], [7], [8], [9]. The watermarking algorithms developed in these works are robust against lossy compression operations, particularly against JPEG 2000, which is developed based on wavelet transform.

In many applications, simultaneous usages of two wavelets are found appropriate where they form an approximate Hilbert transform pairs. Typical applications include transient detection [10], turbulence analysis [11], and waveform encoding [12] etc. Hilbert transform pairs of wavelets are also useful for implementing complex and directional wavelet transforms [13]. Steerable filter [14]-[15] is also designed using Hilbert transform. Kingsbury's complex dual-tree DWT [16], [17] is based on (approxi-

mate) Hilbert pairs of wavelets. Maity et al. developed discrete Hilbert transform pairs using wavelets [18] and proposed an algorithm for capacity improvement in spread spectrum (SS) image watermarking [19]. In all such applications, efficient realization of Hilbert transform significantly improves the performance. Moreover, algorithmic design often demands ease of hardware realization in order to meet real time implementation of the applications.

This work mainly focuses on development of an efficient realization of Hilbert transform pairs using biorthogonal wavelets. Approximate Hilbert transform pair generated from biorthogonal wavelet bases can reduce the computation time efficiently due to symmetric coefficients of the filters. Moreover biorthogonal wavelet filters of linear phase can also be designed. Filter of rational coefficients are then obtained by adjusting the parameters near the optimal values. Approximation to rational coefficients simplifies hardware realization and is verified through its digital design. The novelty of the proposed algorithm is then studied in watermarking application where the concept of QCM of communication theory has been borrowed to increase payload capacity coupled with spread spectrum (SS) modulation technique. Interference rejection attribute of SS has been made use to achieve robustness against common signal processing applications. Simulation results show that biorthognal wavelet based Hilbert transform reduces computation time significantly. It is also shown that Hilbert transform with rational coefficients is easily implemented through hardware. QCM-SS modulation based digital image watermarking algorithm, developed using proposed Hilbert transform, causes marginal perceptual quality degradation of the original image even after two times increase in embedding capacity. Simulation results also show that both the watermarks are affected equally for a particular degradation simulated over the watermarked images.

The rest of the paper is organized as follows: Section 2 describes wavelet based Hilbert transform while Section 3 develops digital design with rational filter coefficients. Section 4 discusses QCM-SS watermarking scheme for digital images. Performance of Biorthoganl wavelet based Hilbert transform, hardware design and QCM-SS watermarking are reported in Section 5 while Conclusions are drawn in Section 6 along with scope of future work.

## 2. Wavelet Based Hilbert Transform

It is already mentioned that two wavelet bases are used in many applications where one wavelet is (approximately) the Hilbert transform of the other. The important question is how one can choose lowpass filters $h_0$ and $g_0$ so that the two wavelets will form a Hilbert transform pair.

Let us recall the definition of Hilbert transform. $\Psi_g(t)$ is the Hilbert transform of $\Psi_h(t)$, if

$$\hat{\psi}_g(w) = \begin{cases} -j\hat{\psi}_h(w), & w > 0 \\ j\hat{\psi}_h(w), & w < 0 \end{cases} \tag{1}$$

In [13], I. W. Selesnick established the relation among $\Phi_g(t)$ and $\Phi_h(t)$, $G_1(w)$ and $H_1(w)$, $\Psi_g(t)$ and $\Psi_h(t)$ assuming that the two lowpass filters are related as follows:

$$G_0(w) = H_0(w)e^{-j\theta(w)} \tag{2}$$

where $\theta(w)$ is $2\pi$ periodic and the symbols $\Phi$ and $\Psi$ denote scaling and wavelets. Let $G(w)$ and $H(w)$ are the Fourier transform of $g(t)$ and $h(t)$ respectively. The relation among the above mentioned pairs are established in the paper [13] as follows:

$$\phi_g(w) = \frac{\phi_g(0)}{\phi_h(0)}\phi_h(w)e^{[-j\sum_{k=1}^{\infty}\theta(\frac{w}{2^k})]}, \tag{3}$$

$$G_1 = H_1 e^{j\theta(w-\pi)}, \tag{4}$$

and

$$\psi_g(w) = \phi_h(w)e^{[j\sum_{k=1}^{\infty}\theta(\frac{w}{2}-\pi)-\sum_{k=2}^{\infty}\theta(\frac{w}{2^k})]}. \tag{5}$$

If $H_0(w)$ and $G_0(w)$ are lowpass CQF (conjugate quadrature filter) with

$$G_0(w) = H_0(w)e^{-j(w/2)}, \text{ for } |w| < \pi \tag{6}$$

the corresponding wavelets are Hilbert transform pairs, i.e. $\psi_g(t) = H[\psi_h(t)]$.

Equivalently, the digital filter $g_0(n)$ is a half-sampled delayed version of $h_0(n)$

$$g_0 = h_0(n-1/2). \tag{7}$$

As a half-sample delay cannot be implemented with FIR (finite impulse response) filter, it is necessary to make an approximation.

Now, based on the number of zero wavelet moments and the parameter for controlling the half-sample delay approximation, a set of design equations need to be solved for the design of the filters $h_0$ and $g_0$ of minimal length. The filter coefficients, for an example, can be found as in Tab. 1 where $N$, $L$ and $K$ denote the length of the wavelet filter, parameter for controlling the half-sample delay approximation and the number of zero wavelet moments respectively. Filter 1 denotes this filter in this paper.

| $h_0$ (n) | $g_0$ (n) |
|---|---|
| 0.03221257407420 | 0.01123179664593 |
| 0.00820937853576 | 0.0293846247110 |
| -0.06023981115681 | -0.02941520794631 |
| 0.2973132183851 | 0.05228807988494 |
| 0.79149943086392 | 0.56614863255854 |
| 0.51279103306800 | 0.77383926442488 |
| -0.05414137333876 | 0.21123282805692 |
| -0.11999180398584 | -0.16831623167690 |
| -0.00222403925601 | -05209126812854 |
| -0.00872685173012 | 0.01991104128252 |

**Tab. 1.** Filter coefficients of Hilbert transform approximately for $N$=10, $K$=4, $L$=5.

The shortcomings of the method are that the designed wavelet filters are always of the same length (even for different values of *K* and *L*) and non-linear phase for the restriction of approximation degree at zero. Better approximation to Hilbert transform pairs requires longer length of wavelet filter band and a much higher order equations to solve in design and more computation cost in applications.

In this paper, the above mentioned design problems of Hilbert transform are taken care using biorthogonal wavelet bases.

If $[H_0(z), H_1(z); \tilde{H}_0(z), \tilde{H}_1(z)]$, $[G_0(z), G_1(z); \tilde{G}_0(z), \tilde{G}_1(z)]$ are the biorthogonal wavelet filter banks, then the following two relations are equivalent.

$$(i)\psi_g(t) = H[\psi_h(t)]; \tilde{\psi}_g(t) = -H[\tilde{\psi}_h(t)],$$

$$(ii)\hat{G}_0(w) = e^{-j(w/2)}\tilde{H}_0(w) \text{ and, } |w| < \pi.$$

If biorthogonal wavelets $\psi_h(t)$, $\tilde{\psi}_h(t)$ and $\psi_g(t)$, $\tilde{\psi}_g(t)$ form a Hilbert transform pair, the corresponding scaling filter pairs have the following relationship:

$$G_0(z) = z^{-1/2}H_0(z),\ \tilde{G}_0(z) = z^{1/2}\tilde{H}_0(z)$$

$$\text{or } g_0 = h_0(n-1/2),\ \tilde{g}_0 = \tilde{h}_0(n+1/2)$$

where $\{h_0(n)\}$ are the coefficients or responses of $H_0(z)$.

If we assume $[H_0(z), \tilde{H}_0(z)]$ and $[G_0(z), \tilde{G}_0(z)]$ are FIR filters, and both satisfy the corresponding PR (perfect reconstruction) condition $P(z)+P(-z)=2$, where $P(z) = H_0(z)\tilde{H}_0(z)$, filter coefficients can be found by minimizing the following relation:

$$\int_0^{\pi} \left( \left|\hat{E}(w)\right|^2 + \left|\hat{\tilde{E}}(w)\right|^2 \right) dw \tag{8}$$

where $\hat{E}(w) = \hat{G}_0(2w) - e^{-jw}\hat{H}_0(2w)$ and

$$\hat{\tilde{E}}(w) = \hat{\tilde{G}}_0(2w) - e^{jw}\hat{\tilde{H}}_0(2w).$$

The better approximate to Hilbert transform pair is achieved when $E(z)$ is closer to zero. If the analysis and the synthesis part is considered separately, the objective function (8) can be replaced by

$$\min_{\alpha} \int_0^{\pi} \left( \left|\hat{E}(w)\right|^2 \right) dw \tag{9}$$

where $\alpha$ denotes the parameter set of biorthogonal wavelet filters to be designed. The optimal parameter $\alpha^*$ determines $H_0(z), \tilde{H}_0(z), G_0(z), \tilde{G}_0(z)$ and wavelet functions can be obtained from scaling and wavelet equations. Let us assume the following values for *L* and *K*.

$$(L_h, \tilde{L}_h) = (7,9), (L_g, \tilde{L}_g) = (8,9); (K_h, \tilde{K}_h) = (5,1) and (K_g, \tilde{K}_g) = (5,1)$$

The filter coefficients are calculated according to the algorithm proposed in [20], [21]. In the paper, we denote these two filters as Filter 2 and Filter 3 and the coefficients are shown in Tab. 2.

The filter coefficients of Tab. 1 and Tab. 2 show that the wavelet functions are smoother in case of biorthogonal wavelet bases. Furthermore, the coefficients of filters in Tab. 2 are symmetric, while in Tab. 1 are asymmetric. These properties are quite advantageous to the various signal processing applications where shorter length and symmetric coefficients of filters can reduce the computation efficiently to about one third of the original.

| $h_0(n)$ | $\tilde{h}_0(n)$ | $g_0(n)$ | $\tilde{g}_0(n)$ |
|---|---|---|---|
| 0 | 0.0095 | 0 | 0.0428 |
| -0.0125 | 0.0264 | -0.0200 | -0.0615 |
| 0.0375 | -0.2321 | -0.0287 | -0.1272 |
| 0.2625 | 0.2216 | 0.1363 | 0.6458 |
| 0.4250 | 0.9454 | 0.4125 | 0.6458 |
| 0.2625 | 0.2216 | 0.4125 | -0.1271 |
| 0.0375 | -0.2321 | 0.1363 | -0.0615 |
| -0.0125 | 0.0284 | -0.0287 | 0.0428 |
| 0 | 0.0095 | -0.0200 | 0 |

**Tab. 2.** The scaling filter coefficients of biorthogonal wavelet bases forming a Hilbert transform approximately.

| $h_0(n)$ | $\tilde{h}_0(n)$ | $g_0(n)$ | $\tilde{g}_0(n)$ |
|---|---|---|---|
| 0 | 19/256 | 0 | 1/32 |
| -1/128 | 57/128 | -1/64 | -1/32 |
| 3/64 | -11/4 | -1/64 | -7/32 |
| 33/128 | 263/128 | 9/64 | 23/32 |
| 13/32 | 1325/128 | 25/64 | 23/32 |
| 33/128 | 263/128 | 25/64 | -7/32 |
| 3/64 | -11/4 | 9/64 | -1/32 |
| -1/128 | 57/128 | -1/64 | 1/32 |
| 0 | 19/256 | -1/64 | 0 |

**Tab. 3.** The rational scaling filter coefficients of biorthogonal wavelets form Hilbert transform pair approximately.

Furthermore, the coefficients of two filter banks can be approximated to rational numbers, and their approximation to Hilbert transform pair is almost unchanged. It is possible to approximate optimized parameters $\alpha$ while solving the function (9) by some rational values so that the coefficients of two filter banks are all rational numbers. Tab. 3 shows rational scaling filter coefficients and is denoted by Filter 4 and Filter 5 in this paper. Since the filter coefficients have the values with denominators in the form of $2^k$, $k \in$ z, computation for wavelet transform becomes easy requiring only addition and shift operations. The rational filter coefficients greatly simplify hardware design and are discussed in the next section.

## 3. Hardware Design

Digital circuit is developed for one-dimensional input signal. It is assumed that each input is of 8-bits so as to represent the pixel values of a monochrome image, number of filter coefficients 9 (based on the design), number of bits allocated to represent the coefficient is 9 (one bit for sign and eight bits for magnitude).

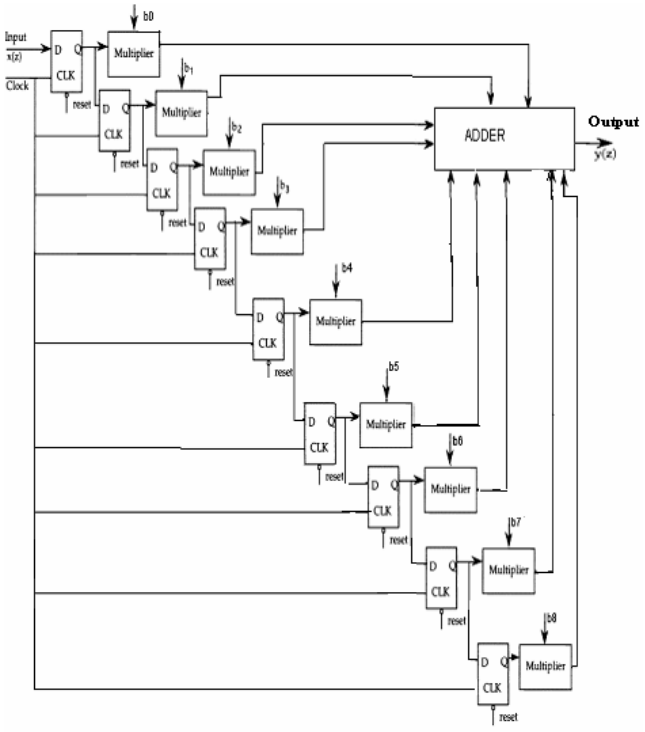


**Fig. 1.** Block circuit of analysis filter bank where b0-b8 are the coefficients of the filter.

The detailed architecture for the wavelet analysis is depicted in Fig. 1. The characteristics of such a filter are determined by a set of coefficients $h_0, \ldots, h_n$ applied respectively to each of the multipliers. Variation in the values of these coefficients allows the designer to control the characteristics of the wavelet transform operation. The multiplication is carried out using simple shift-and-add multiplier blocks. Since the multiplicands are signed, we use 2's complement arithmetic in all mathematical operations. It is observed that the denominators of all coefficients can be expressed in powers of 2. Hence the division operation can easily be accomplished using parameterized right-shifter blocks. Thus we have a right-shifter block tailing every multiplier unit in the filter bank design units. Although digital design of wavelet filter bank analysis is shown in Fig. 1, the same for the synthesis part is also identical except wavelet coefficients are the input here and the corresponding outputs are the signal values in space or time domain, i.e. in original domain.

It is to be noted that the addition of a stream of zeroes between every two consecutive samples cannot be avoided. The buffer/latch is necessary for synchronization purposes and its length is equal to the data word length which is 8-bit in this case. The bi-orthogonal wavelet based Hilbert transform makes use of 9-tap high precision floating-point filter coefficients. Hence filtering operations during analysis and synthesis make estimation of the required memory resources difficult and consequently makes the design highly complicated. One possible solution to this problem is to approximate the coefficients of the filter banks as rational numbers such that no significant loss in signal integrity is encountered. Therefore in this design, we use rational numbers as filter coefficients.

The circuit diagram of the 9-tap low pass analysis filter bank is shown in Fig. 1. Since there are 9 filter coefficients, the hardware implementation needs 9 multipliers, 9 D flip-flops and one 16-bit signed adder unit. The circuit of decimation (down-sampling) and interpolation (up-sampling) are shown in Fig. 2. In the decimator, a D flip-flop is used and the clock rate of the input must be equal to half the clock of the D flip-flop so that only every alternate input to the decimator is fed to the interpolator unit. In the interpolation block, i.e. the up-sampling block, the clock rate of the input must be equal to twice that of the clock for the D flip-flop so that a zero is inserted between every two successive inputs to the Up-sampling block. Circuit models for the decimator and interpolator are shown in Fig. 2.

To keep the scalability feature of the architecture at a stage level, some considerations need to be made (Even if only the analysis is discussed, the approach is also valid for the synthesis). The possible scheme is to preserve the data word-length. In this scheme, the filtered and the decimated data need to be truncated to the same data word-length (the initial data word-length). To fulfill the truncation requirement, the clock used for providing data words as inputs needs to be set to zero (frozen) for an adequate number of cycles (according to the internal word-length). The control circuitry follows simple and regular design rules. It is to be mentioned that if the data word-length resulting from a filtering and decimating process is different from the original one, the scalability is lost.

This circuit design model can be extended to design a Hilbert transform system to process 2-D signals like still images. A possible circuit model for such a system is suggested in Fig. 3.

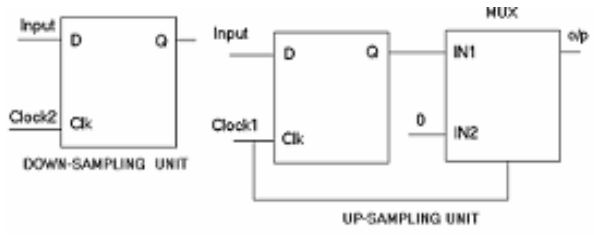


(a) (b)

**Fig. 2.** Circuit diagram for (a) down sampling and (b) up sampling unit.

After developing Hilbert transform pairs and its digital design, our objective is to study the performance of Hilbert transform pairs, i.e. to verify how efficient is the

design of this Hilbert transformation. This task has been accomplished here through the performance analysis of QCM-SS image watermarking proposed in this work. The QCM-SS watermarking method is discussed in the next section.

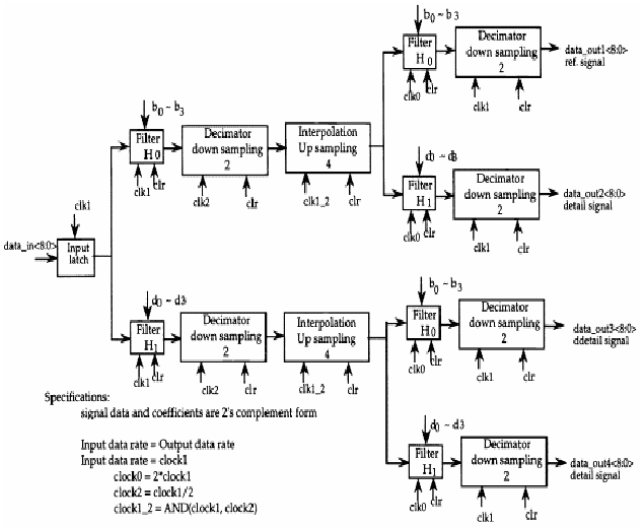


**Fig. 3.** Circuit block diagram for 2-D Hilbert transform analysis.

# 4. QCM-SS Watermarking

Digital watermarking problem has been viewed from different angles by different researchers and becomes a multidisciplinary research area. Among them, the popular and widely used approach is based on theory of communication where the watermark is considered as a signal to be transmitted. Accordingly, modulation and multiplexing techniques are used widely for designing watermarking algorithms [22]. In communication, quadrature carrier multiplexing (QCM) is used to transmit two message signals using the same carrier with phase quadrature. This principle has been made use here for doubling the payload capacity in digital watermarking. Furthermore, SS principle has been incorporated to meet robustness requirement. Robust and high capacity SS watermarking can be designed if image signal is decomposed in proper directions so that low correlation value with the code patterns can be achieved in each decomposition. It has been reported in [23] that biorthogonal wavelet decomposition, possibly due to the complementary information of the two wavelet systems, offers better directional selectivity compared to classical wavelet transform and yields lower correlation with the code patterns.

Thus development of QCM-SS watermarking principle demands efficient realization of Hilbert transformation. To study the performance of the proposed biorthogonal wavelet transform, we propose QCM-SS watermarking for digital images. Two watermark signals can be embedded by decomposing the cover image using Hilbert transform pairs. The proposed QCM-SS watermarking scheme, like other conventional watermarking schemes, consists of two parts namely watermark embedding and watermark decoding.

## 4.1 Watermark Embedding

We consider a gray scale image as cover or test image and a binary image as watermark information. Watermark embedding process consists of the following steps.

*Step 1: Decomposition of cover image*

The cover image is decomposed in two different directions using the filter coefficients given in Tab. 2 or Tab. 3.

*Step 2: Formation of message vector*

Let $(M\times N)$ be the size of the binary watermark message, which is converted into a vector of size $[(M.N)\times 1]$, called as message vector. Each element of the message vector is either '1' or '0'. The total number of bits of the message vector is $M.N$.

*Step 3: Generation of code patterns*

The widely used code pattern for SS modulation technique is pseudo noise (PN) sequence. The size of the PN sequence is identical to the size of the wavelet coefficient matrix. Thus a set of PN matrices denoted by $(P_i)$ of number $(M.N)$ are generated and is modulated by Walsh-Hadamard (W-H) matrix [24]. Performing exclusive-OR operation of code pattern with W-H matrix does the modulation.

*Step 4: Watermarked image formation*

The modulated code pattern $PN_a$ is used to embed data in the LL (low-low) subband. An orthogonal code pattern $PN_d$ is obtained by complementing the bits of $PN_a$ and is used for data embedding in the HH (high–high) subband. To improve robustness in binary modulation, antipodal embedding scheme is used. So the data embedding rule can be expressed as follows:

$$X^{e} = \begin{cases} X + K\,.P_i \\ X - K\,.P \end{cases} \tag{10}$$

Here '+' and '-' in (10) are used when the watermark bit '$b$'=1 or 0 respectively. The symbol $X$ represents the wavelet coefficient of the cover image, $X^e$ is the wavelet coefficient after watermark embedding, $K$ is the modulation index, $P_i$ is the set of PN matrices. Two different binary watermarks are embedded in two different decomposition of the cover obtained by using two different Hilbert transforms. Quadrature decomposition, due to orthogonality, allows the use of single set of spreading codes for embedding two watermarks in the same cover. After watermark bit embedding inverse wavelet transform is done to obtain the watermarked image.

## 4.2 Watermark Decoding

The watermark recovery process requires the set of PN matrices ($Pi$) that were used for data embedding. Different steps for watermark decoding are described as follows:

*Step 1: Watermarked image decomposition*

The watermarked image or its possibly distorted version is decomposed using the same biorthogonal wavelet based Hilbert transform pairs of Tab. 2 or Tab. 3.

*Step 2: Correlation calculation*

To decode message bit, two correlation values between the watermarked wavelet coefficients and the code patterns (one from LL and other from HH sub band) are calculated. Total *M.N* (total number of watermark bits) number mean correlation values $\mu_i$'s are obtained where $i$=1, 2,.. {*MxN*}.

*Step 3: Mean correlation calculation and threshold selection*

From these mean correlation values, we calculate an overall mean correlation value ($T$) that is used as the threshold for watermark decoding. The decision rule for the decoded watermark bit is as follows:
(i) for $\mu_i \geq T$, the extracted bit is 1,
(ii) for $\mu_i < T$, the extracted bit is 0.

# 5. Performance Evaluation

We present performance evaluation of the proposed work in three different subsections. Section 5.1 highlights novelty of the proposed Hilbert transform and the performance comparison with the work [13]. Then the results of digital design are presented in Section 5.2. Finally performance of the proposed QCM-SS watermarking and comparison with [27] is reported in Section 5.3.

## 5.1 Performance of Biorthogonal Wavelet Based Hilbert Transform

We first consider a sinusoidal signal as input test signal. Performances of Hilbert transformations are compared in terms of computation time required and Mean Square Error (MSE) that represent error in approximation. It is expected that lower the value of MSE, better is the approximation. Similarly, lower the time required for computation, efficient is the filter realization and is well suited for real time applications. We perform experiment using visual C/C++ running on a Pentium III 400 MHz PC system.

Simulation results shown in Tab. 4 indicate that Hilbert transform obtained from limit functions defined by the infinite product formula (Filter 1) has the best output, i.e. the minimum error, but requires the largest computation time. This has been shown by the numerical values shown in column 2 and column 3 of Tab. 4. It is also observed that if the number of points in the input sequence increases, MSE also decreases.

Tab. 5 shows performance for an arbitrary sinusoidal signal using Filter 3 and Filter 4. Results in Tab. 4 and Tab. 5 indicate that the computation time of Filter 2 and Filter 3 are almost the same but the former shows better output compared to the latter. The difference in output performance of Hilbert Transform pair (Filter 2 and Filter 3) is seen due to energy imbalance for the coefficients of two biorthogonal wavelets.

| No. of points | Comp. Time (ms) | MSE | Comp. Time (ms) | MSE |
|---|---|---|---|---|
| 11 | 0.1560 | 0.4338 | 0.0930 | 0.7288 |
| 31 | 0.1780 | 0.4143 | 0.1250 | 0.6739 |
| 51 | 0.3130 | 0.2234 | 0.1870 | 0.5271 |
| 71 | 0.5470 | 0.11231 | 0.2810 | 0.4268 |
| 91 | 0.7650 | 0.0954 | 0.4060 | 0.3623 |
| 101 | 0.8480 | 0.0145 | 0.5123 | 0.3398 |

**Tab. 4.** Shows performance for Filter 1 and Filter 2 where numerical values in columns 2 and 3 indicate performance of Filter 1 and columns 4 and 5 for Filter 2.

| No. of points | Comp. Time (ms) | MSE | Comp. Time (ms) | MSE |
|---|---|---|---|---|
| 11 | 0.0940 | 0.7514 | 0.0213 | 0.7643 |
| 31 | 0.1260 | 0.7072 | 0.0432 | 0.7201 |
| 51 | 0.1880 | 0.5577 | 0.0543 | 0.5813 |
| 71 | 0.2820 | 0.4534 | 0.0753 | 0.4998 |
| 91 | 0.4120 | 0.3957 | 0.0848 | 0.4213 |
| 101 | 0.5230 | 0.3606 | 0.0901 | 0.3923 |

**Tab. 5.** Shows performance for Filter 3 (columns 2 and 3) and Filter 4 (columns 4 and 5).

| Input sequence length | PSNR in (dB) for floating coefficients | PSNR in (dB) for rational filter coefficients |
|---|---|---|
| 10 | 34.20 | 30.93 |
| 20 | 36.88 | 33.12 |
| 30 | 45.87 | 42.65 |
| 40 | 46.88 | 44.13 |
| 50 | 50.40 | 48.28 |
| 100 | 56.71 | 53.87 |

**Tab. 6.** Shows performance for the floating and the rational filter coefficients.

The computation time required for Filter 4 (or Filter 5) is the smallest among all the filters and is shown by the values in column 4 of Tab. 5. Results in Tab. 5 also show that computation time decreases using biorthogonal wavelet based rational Hilbert transform coefficients and at the same time degradation in signal reconstruction is well within the acceptable limit. Also a comparative study of the simulation results for an arbitrary sequence is shown using floating point and rational filter coefficients. Tab. 6 shows that PSNR (peak signal-to noise ratio) drops very slightly for rational coefficients, but the loss in signal integrity remains within appreciable limits. It is also observed that the performance of the system improves significantly when the input sequence length is more i.e. when we provide more inputs to the system.

| Logic utilization | Used | Availability | Utilization |
|---|---|---|---|
| No. of slices | 1537 | 1920 | 80% |
| No. of slice FF | 811 | 3840 | 21% |
| No. of 4 input LUT | 1005 | 3840 | 26% |
| No. of bonded IOB | 26 | 173 | 15% |
| No. of GCLKs | 3 | 8 | 37% |
| No. of CLBs | 58 | 1296 | 4.4% |

**Tab. 7.** shows device utilization (target device- xc4036).

## 5.2 Digital Design Performance

To assess the effectiveness of the digital design, a single level of 1-D biorthogonal Hilbert transform pair, has been designed using Verilog HDL (hardware description language) and is implemented on the Xilinx XC4036 FPGA (field programmable gate array) [25]. The XC4036 consists of 36x36 arrays of Configurable Logic Blocks (CLB). The input data and the multiplier are 8-bits and 9-bits in lengths. To get a compact layout and an optimal clock speed, the placement and timing constraints have been added to the design. The implementation report shows that a DWT stage occupies 58 CLBs for a frequency of 100 MHz**.** Functional and timing simulations have been carried out by means of the Xilinx Software tool (Foundation 2.1i).

The device usage is normally reported in terms of number of look-up tables, I/O buffers, and flip-flops. The routing resource usage is not given by the place and route tools - a higher device utilization implies a greater routing resource utilization. The total numbers of CLBs used are a function of the device resources used and how densely they are packed. For example, on a CLB only a flip-flop could be used, but still it adds to the CLB count. The usages are given in Tab. 7.

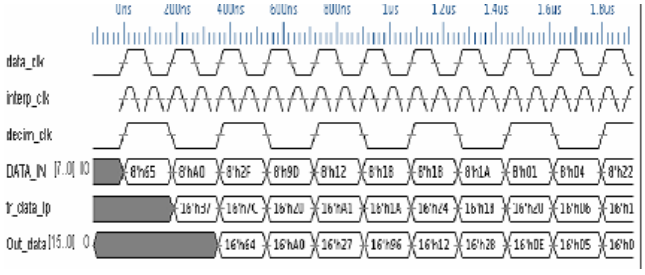


(a)

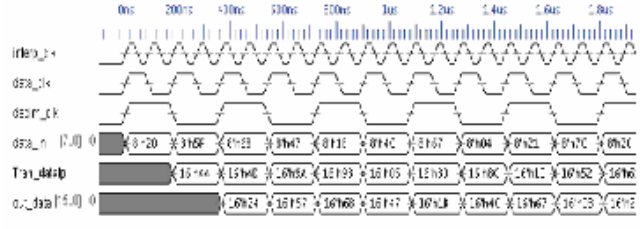

(b)

**Fig. 4.** Timing diagram (a) for Filter 4 and (b) for Filter 5.

It is observed from the timing diagrams shown in Fig. 4 (a) and Fig.4 (b) that the Hilbert transform system is capable of analyzing and reconstructing the signals with appreciable accuracy.

## 5.3 Performance of QCM-SS Watermarking

The watermarks are binary images of size (16 x 16) and the cover image is a gray-scale image of size (256 x 256), 8 bits/pixel. The proposed algorithm requires approximately 5 seconds for watermark embedding and approximately 3 second for watermark extraction using the filter coefficients of Tab. 2 in Visual C/C++ platform running on a Pentium III 400 MHz PC system. This computation time is further reduced significantly when rational filter coefficients of Tab. 3 are used. The watermark embedding and decoding process requires 11 seconds for embedding and 7 seconds for decoding in the same computation platform using the filter coefficients of Tab. 1. In this paper, we use both Peak Signal to Noise Ratio (PSNR) [24] and mean Structural SIMiliarity index (MSSIM) [26] to quantify imperceptibility of the hidden data. MSSIM is the mean of the SSIM values and represents image quality by a single numerical value with its highest value 1 corresponding to no distortion. Fig. 5(a) shows the test image Fishing Boat of size (256 x 256) and binary watermark images are shown in Figs. 5(b)-5(c) with size (16 x 16). Figs. 5(d) and 5(e) show the watermarked images after embedding two watermarks using filter coefficients of Tab. 2 and Tab. 1, respectively. It is to be noted that images shown in Fig. 5(d) and 5 (e) are visually indistinguishable with respect to the original image shown in Fig. 5(a) which highlights the novelty of the usage of wavelet based QCM-SS watermarking in satisfying the imperceptibility property of watermarking. Similarly, the visual indistinguishable nature between Fig. 5(d) and 5(e) shows that the proposed biorthogonal wavelet based Hilbert transform pair design does not cause much loss in signal reconstruction with respect to the filters shown in Tab. 1. This subjective quality difference is supported by PSNR values (objective measure) which are 36.06 dB and 36.14 dB respectively for Fig. 5(d) and Fig. 5(e) with respect to Fig. 5(a).

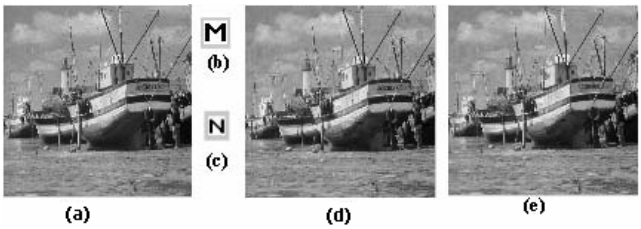


**Fig. 5.** (a) Test image, (b)-(c) watermark images, (d) watermarked images after embedding two watermarks using coefficients of Tab. 2, (e) watermarked images after embedding two watermarks using coefficients of Tab. 1.

Although the experiment has been performed over large number of cover images, however, Tab. 8 shows the effect of two messages embedding on data imperceptibility for the few cover images. Numerical values in columns 2 and

columns 3 indicate visual quality measures of the watermarked images after single watermark embedding while values shown in column 4 and column 5 indicate the same after two watermarks embedding. The results show that even in two times increase in payload capacity, visual quality does not change significantly. This highlights the novelty of QCM method.

| Test Images | PSNR (dB) after single | MSSIM after single | PSNR (dB) after two | MSSIM after two |
|---|---|---|---|---|
| Lena | 35.47 | 0.9536 | 35.45 | 0.9514 |
| Boat | 36.12 | 0.9632 | 36.06 | 0.9612 |
| Pills | 34.23 | 0.9454 | 34.09 | 0.9423 |
| Opera | 36.78 | 0.9645 | 36.56 | 0.9634 |

**Tab. 8.** Data imperceptibility after embedding two different binary watermark images of size (16 x 16).

The results in Tab. 9 show that visual distortion after embedding two watermarks is much lower in the proposed method compared to [27] as it is found that PSNR values after embedding two messages are 36.06 dB for the present algorithm and 31.06 dB for the latter algorithm.

| Test Images | PSNR (dB) after single | MSSIM after single | PSNR (dB) after two | MSSIM after two |
|---|---|---|---|---|
| Boat | 36.12 | 0.9632 | 36.06 | 0.9612 |
| Boat | 36.27 | 0.9645 | 31.06 | 0.9132 |

**Tab. 9.** Comparison of data imperceptibility; the first row for the proposed method and the last row for the method in [27].

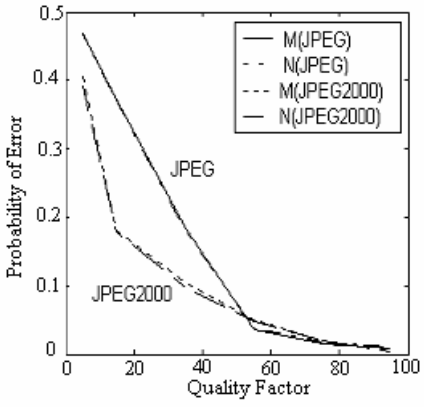


**Fig. 6.** Robustness performance against JPEG and JPEG 2000 compression operations for the two watermarks embedded in two quadrature decompositions.

We have evaluated the performance of the proposed technique in several compression frameworks. However, we present here only the results corresponding to JPEG and JPEG 2000 compression framework. Fig. 6 shows the robustness performance of two messages embedding against JPEG and JPEG 2000 compression operations. At a particular quality factor, probability of decoding error for both the watermark images are almost the same for a given compression framework. This indicates that QCM watermarking scheme offers the same robustness performance for the watermarks embedded in two decompositions leading to the better design of Hilbert transform pairs. As expected, due to wavelet domain embedding, robustness performance of the proposed algorithm against JPEG 2000 compression is better compared to JPEG compression. This is indicated in Fig. 6 by low probability of error values for the decoded watermarks in case of JPEG 2000.

Fig. 7 shows the robustness performance of the proposed algorithm against additive gaussian noise. Robustness performance is decreased with the increase of the variance value of the noise. As expected, QCM watermarking scheme offers the similar performance variation for both the decoded watermarks when watermarked images are corrupted by additive noise. This once again supports the efficiency of the proposed Hilbert transform design.

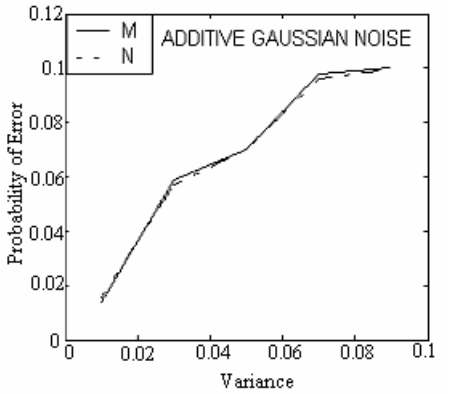


**Fig. 7.** Robustness performance against additive gaussian noise operations for the two watermarks embedded in two quadrature decompositions.

## 6. Conclusions and Future Works

This paper proposes a novel algorithm for approximate Hilbert transform pair generation from biorthogonal wavelet bases. The algorithm reduces computation time significantly due to symmetric coefficients of the filter while performance is comparable with respect to other existing algorithms. Moreover biorthogonal wavelet filters of linear phase can also be designed. Filter of rational coefficients for Hilbert transform pairs can be obtained by adjusting the parameters near the optimal values and such type of design leads to simpler hardware realization. Digital design for 1-D signal is developed and highlights suitability of the algorithm for many real-time multimedia signal processing applications. Finally, this Hilbert transform pairs is used to realize quadrature carrier multiplexing scheme with an application to spread spectrum image watermarking. QCM principle increases data embedding rate twice with negligible loss in image quality and almost no robustness performance degradation. It is also found that watermarks embedded in two quadrature decompositions are affected in the similar fashion when various signal processing operations are simulated over the watermarked images and highlights the novelty of the proposed algorithm developed for generation of Hilbert transform pairs.

Future work may be carried out to study the performance of the proposed Hilbert transform pairs for other applications such transient detection, turbulence analysis and waveform coding etc. Development of a dedicated chip for QCM-SS image watermarking may also be taken as a future research work.

## References


[1] PROAKIS, J. G., MANOLAKIS, D. G., SARMA, D. *Digital Signal Processing*. New Delhi: Pearson Education, 2006.

[2] HAYKIN, S. *Communication Systems*. 3rd ed. Singapore: John Wiley & Sons, 1995.

[3] BURRUS, C. S., GOPINATH, R. A., GUO, H. *Introduction to Wavelets and Wavelet Transforms, A Primer*. New Jersey: Prentice Hall, 1997.

[4] PENNEC, E. L., MALLAT, S. Sparse geometric image representations with bandelets. *IEEE Transactions on Image Processing,* 2005, vol. 14, no. 4, p. 423-438.

[5] MEERWALD, P., UHL, A. A survey of wavelet domain watermarking. In *Proceedings of SPIE, Electronic Imaging, Security and Watermarking of Multimedia Contents III*, vol. 4314, 2001.

[6] COX, I. J., KILIAN, J., LEIGHTON, F. T., SHAMOON, T. Secure spread spectrum for multimedia. *IEEE Transaction on Image Processing*, 1997, vol. 6, p. 1673–1687.

[7] LANGELAAR, G. C., SETYAWAN, I., LAJENDIJK, R. L. Watermarking in digital images and video data. *IEEE Signal Processing Magazine*, 2000, vol. 17, p. 20–46.

[8] GROBOIS, R., EBRAHIMI, T. Watermarking in JPEG 2000 domain. In *Proc. of the IEEE Workshop on Multimedia Signal Processing*, 2001, p. 3–5.

[9] MAITY, S. P., KUNDU, M. K. A blind CDMA image watermarking scheme in wavelet domain. In *Proceedings of IEEE International Conference on Image Processing*, 2004, p. 2633–2636.

[10] ABRY, P., FLANDRIN, P. Multiresolution transient detection. In *Proc. of IEEE-SP Int. Symp. Time-Frequency, Time-Scale Analysis*, 1994, p. 225–228.

[11] ABRY, P. *Ondelettes et Turbulences*. Paris, France: Diderot, 1997.

[12] OZTURK, E., KUCUR, O., ATKIN, G. Waveform encoding of binary signals using a wavelet and its Hilbert transform. In *Proc. of IEEE Int. Conf. on Acoust., Speech, Signal Process.*, June 5–9, 2000.

[13] SELESNICK, I. W. Hilbert transform pairs of wavelet bases. *IEEE Signal Processing Letter*, 2001, vol. 8, p. 170–173.

[14] FREEMAN, W. T., ADELSON, E. H. The design and use of steerable filters. *IEEE Transaction on Pattern Analysis and Machine Intelligence*, 1991, vol. 13, p. 891–906.

[15] SIMONCELLI, E. P., FREEMAN, W. T. The steerable pyramid: A flexible architecture for multi-scale derivative computation. In *Proc. of IEEE International Conference on Image Processing*, 1995.

[16] KINGSBURY, N. G. The dual-tree complex wavelet transform: A new technique for shift invariance and directional filters. In *Proceedings of the Eighth IEEE DSP Workshop*, 1998.

[17] KINGSBURY, N. G. A dual-tree complex wavelet transform with improved orthogonality and symmetry properties. In *Proceedings of IEEE Int. Conference on Image Processing*, 2000.

[18] MAITY, S. P., MAITY, S. Design of Hilbert transform using discrete wavelet. In *Proceedings of Int. Conference on Computers and Devices for Communication (CODEC-2006),* Kolkata (India), 2006.

[19] MAITY, S. P., KUNDU, M. K., MAITY, S. Capacity improvement in digital watermarking using QCM scheme. In *Proc. of the 12th National Conf. on Communications, IIT Delhi*, 2006, p. 511-515.

[20] CHENG, L., WANG, H. The solution of III- conditioned stoeplitz systems via two-grid and wavelet method. *Comp. Math. Appl.,* 2003, vol. 46, no. 6.

[21] CHENG, L., XIANG, D. General construction of 9/7 wavelet filter and its application in image compression. *Optical Engineering*, 2003, vol. 42, no. 8.

[22] BAUDRY, S., DELAIGLE, J. F., SANKUR, B., MAITRE, H. Analysis of error correction strategies for typical communication channel in watermarking. *Signal Processing*, 2001, vol. 81, no. 6, p. 1239-1250.

[23] MAITY, S. P., KUNDU, M. K., DAS, T. S. Robust SS watermarking with improved capacity. *Pattern Recognition Letters, 2007,* vol. 28, p. 350-356.

[24] GONZALEZ, R. C., WOODS, R. E. *Digital Image Processing*. 2nd ed. Singapore: Pearson Education Inc., 2002.

[25] SCHONER, B., VILLASENOR, J., MOLLOY, S., JAIN, R. Techniques for FPGA implementation of video compression systems. In *Proc. of ACM/SIGBA International Symposium on FPGA*, 1995.

[26] WANG, Z., BOVIK, A. C., SHEIKH, H. R., SIMONCELLI, E. P. Image quality assessment: From error measurement to structural similarity. *IEEE Trans. on Image Processing*, 2004, vol. 13, p. 1–14.

[27] KUNDUR, D., HATZINAKOS, D. A robust digital image watermarking method using wavelet based fusion. In *Proceedings of IEEE International Conf. on Image Processing*, 1997, p. 544-547.


## About Authors …

**Santi Prasad MAITY** received his B.E. in Electronics and Communication Engg. and M.E. degree in Microwaves, both from the University of Burdwan, India in 1993 and 1997 respectively. He submitted his Ph. D thesis in Computer Science & Technology in Bengal Engg. and Science University, Shibpur, India in June 2007. He is working as Assistant Professor at the Dept. of Information Technology, Bengal Engg. and Science University, Shibpur and course coordinator in M.E. in Information and Communication Engg. He also worked as Lecturer in Electronics and Telecommunication Engg. department of the same university from 2000 to 2006. Prior to that, he worked as Lecturer in Electronics and Telecommunication Engg. department of K. G. Engineering Inst., Bishnupur, Bankura, India and Haldia Inst. of Technology, Haldia, India, from 1997 to 2000. His research areas include digital image watermarking, multiuser detection in CDMA, digital signal processing. He delivers several lectures and invited talk on short term course/seminar/workshop/conference and acts as committee member for national and international conferences.

**Seba MAITY** received her M.E. in Electronics and Telecommunication Engg. from the Bengal Engineering and Science University, Shibpur, India in 2004. She is working as Lecturer in Electronics and Communication Engg. department of College of Engineering and Management, Kolaghat, India since 2006. Prior to that she worked as Lecturer in Electronics and Communication department of Hoogly College of Engg. & Technology, Hoogly, India, Calcutta Inst. of Engg. and Management, Tollygunge, India and Narula Institute of Technology, India, from 2004 to 2005. Her areas of teaching and research interest include digital communication, VLSI design and architecture.